BOREAL ENVIRONMENT RESEARCH 18: 488–502
ISSN 1239-6095 (print) ISSN 1797-2469 (online)

Helsinki 2 December 2013

Estimating deep water radiance in shallow water: adapting optical bathymetry modelling to shallow river environments

Claude Flener

Department of Geography and Geology, FI-20014 University of Turku, Finland

Received 3 May 2012, final version received 7 Mar. 2013, accepted 27 Feb. 2013

Flener, C. 2013: Estimating deep water radiance in shallow water: adapting optical bathymetry modelling to shallow river environments. *Boreal Env. Res.* 18: 488–502.

The effect of deep-water radiance on modelling bathymetry in shallow rivers using Lyzenga's algorithm was investigated. To this end, a new method for estimating deep-water radiance in the absence of deep water is presented. This parameter is necessary for applying Lyzenga's optical bathymetry model to aerial photographs and other forms of remotely sensed data. The estimation was tested in the Tana river in northern Finland where the variable in question could be measured as well as estimated, and also in one of the Tana's optically shallow tributaries, where it was necessary to estimate deep-water radiance. The results show that the estimated values are very similar to measured deep-water radiance values in the larger river, but the effect of deep-water radiance in very shallow water seems to be negligible. The new technique described in this paper allows the Lyzenga optical bathymetry model to be employed in clear-water optically-shallow rivers, where deep-water radiance cannot be measured in the field, which is precisely where Lyzenga's model is able to deliver the highest accuracy. The method also provides a reproducible, unbiased method for estimating deep-water radiance even in water deep enough to digitize it manually from remotely sensed data.

Introduction

Recent years have seen developments in the mapping of bathymetry in rivers based on aerial photography and other types of remotely sensed data (Marcus and Fonstad 2008), but it is still not in widespread use. Continuous representation of riverbed topography is important in fluvial geomorphology (e.g., Lane 2000, Wright *et al*. 2000, Lane *et al*. 2003, Alho and Mäkinen 2010), hydrology (e.g., Bates *et al*. 2003), and flood modelling (e.g., Horritt and Bates 2002, Lotsari *et al*. 2010). Aerial imagery-based methods offer the potential to cover larger areas with less effort and cost than boat-based sonar surveys. One of the most commonly used methods for modelling bathymetry in riverine environments is that developed by Lyzenga (1981) based on remotely sensed imagery (e.g., Winterbottom and Gilvear 1997, Westaway *et al*. 2003, Gilvear *et al*. 2007, Flener *et al*. 2012). The Lyzenga model has also inspired the development of related models (Conger *et al*. 2006, Legleiter *et al*. 2009) that aim at overcoming some of its limitations, in particular with regard to substrate variability.

Optical bathymetry models are based on the effect the exponential attenuation of light in water has on the radiance values measured in the remotely-sensed image. The attenuation of light in water is described by the Beer-Lambert law of

Editor in charge of this article: Harri Koivusalo

logarithmic decay, which some models rely on directly (e.g., Carbonneau *et al*. 2006). The Beer –Lambert law describes the exponential attenuation of light in the water:

$$I = I_0 e^{-\beta D} \quad (1)$$

where e is the base of natural logarithms, I is the intensity of light at a certain depth, I_0 is the intensity of light immediately after entering the water (i.e., not including light reflected from the water surface), β is the attenuation coefficient and D is the distance that light travels through water. Lyzenga's algorithm, however, serves to linearize the exponential relationship between depth and radiance using values measured in an image. Conceptually, the model tries to isolate the depth signal in a remotely sensed image by discarding the influences of sediment and other water column constituents on the radiance measured. In order to achieve this, it is necessary to determine the radiance of a location where the water is deep enough for the riverbed not to have any influence on the measured radiance (Stumpf and Holderied 2003). This deep-water radiance is then subtracted, for each spectral band, from the radiance of each pixel in the remotely sensed image. The natural logarithm of the resulting value gives a value X that is linearly related to depth for band i:

$$X_i = \ln(L_i - L_{si}) \quad (2)$$

where L_i is the observed radiance and L_{si} is the deep water radiance in the same band. The model equation is then determined by applying a multiple linear regression of the linearized X_i values to measured depth points. This deep-water correction also serves as a crude way of accounting for atmospheric effects. Because the model was originally developed for coastal bathymetric modelling, the method for obtaining deep-water radiance as described by Lyzenga (1981) consists of simply averaging the pixels from an area far enough removed from the shore, where the water is optically deep. In rivers, particularly in clear water optically shallow rivers where this model is most readily applied, it is often impossible to find an area deep enough to retrieve this parameter (Legleiter *et al*. 2009). While some authors (e.g., Gilvear *et al*. 2007) have measured deep-water radiance in the field, other workers employing this technique in rivers do not specify how they retrieve the deep-water radiance parameter that the model requires (e.g., Winterbottom and Gilvear 1997, Bryant and Gilvear 1999, Lane *et al*. 2003, Westaway *et al*. 2003). While none of these papers specifically mention leaving out the deep-water correction, it raises the interesting question as to whether this omission would be viable in shallow rivers. In rivers, which are relatively shallow compared with the coastal environments the optical bathymetry methods originate from, the contribution of the atmosphere, water surface and water column may be negligible relative to the bottom-reflected radiance (Legleiter *et al*. 2009).

This paper aims to investigate the assumption that deep-water radiance can be ignored in shallow river environments. In order to achieve this, we propose that it is possible to estimate the deep-water radiance parameter, thereby allowing the application of Lyzenga's algorithm in shallow rivers and streams without the need to use in-field spectrometry. Therefore, the aims are (1) to present and test a new deep water radiance estimation algorithm, and (2) to assess whether deep-water radiance can be assumed negligible.

Parameter estimation method

The model developed by Lyzenga (1981) requires aerial imagery and field-based depth measurements as inputs. The measured depth values are used to establish a multiple linear regression to the deep water corrected digital numbers (DN), substituted for radiance, of the remotely sensed image. The deep-water correction is calculated using Eq. 2.

In case the river section to be modelled does not contain any area where deep-water radiance (L_{si}) can be retrieved from the image, it can be estimated by forcing the value to accomplish the goal of reaching a linear relationship between depth and measured radiance. This method is based on the implied assumption in the Lyzenga model, that subtracting L_{si} from the DN values conceptually removes all non-riverbed related information contained in the image, leaving

only depth and substrate effects. The Lyzenga bathymetry model does not account for possible substrate variability. Therefore, assuming uniform substrate throughout the scene, the logarithm of the resulting value X_i should ideally be perfectly linearly related to depth. Hence, any value that, when subtracted from L_{si}, results in X_i being linear relative to measured depth has achieved its conceptual goal of removing non-riverbed information. Based on that observation, deep-water radiance can be computed by starting with a seed value for L_{si} and calculating Pearson's product-moment correlation of the resulting values to depth. If the resulting correlation coefficient (r_p) is approximately equal to –1, the seed value represents a theoretical deep-water radiance. If r_p differs substantially from –1, the seed value is adjusted and the process is repeated until a correlation coefficient close to –1 is achieved. This results in an idealised deep-water radiance value, which should give the same (if not better) bathymetry results than a manually selected L_{si}. Furthermore, the L_{si} values obtained by this reproducible method are more objective than averaged values of manually selected points (i.e., digitised form an image), even where deep water is available.

In order to avoid over-fitting the data, which can cause the residuals to spread unreasonably in order to force a correlation coefficient of –1, it is necessary to compute X_i in each loop of the estimation using the current seed value and stop the estimation once the minimum X_i reaches 0. This avoids L_{si} values being computed that exceed L_i values and hence produces errors caused by attempting to take the logarithm of a negative number when applying Eq. 1. The deep-water estimation process is illustrated by the pseudo-code presented in Appendix, and can be easily implemented in any programming language. The author's implementation of the algorithm is available as part of the river modelling package rivR (http://r-forge.r-project.org/projects/rivr/) in the R software environment for statistical computing.

Note that, while the bathymetry model is calculated as a multiple regression, combining the information of several image bands, L_{si} is estimated for each band separately. In order to assure the estimation is not biased by the data sample, I cross-validated the estimation using 100-fold random sub-sampling using a 70% training set.

Study area

The parameter estimation was tested in a section of the Tana river (Tenojoki in Finnish, Tanaelva in Norwegian), and one of its tributaries, Pulmankijoki, located in the northernmost part of Fennoscandia. The two sites were chosen so as to include one site where the water is deep enough to be able to manually select L_{si} from the images and one site that is optically shallow, representing the target environment for this method.

The Tana is 330 km long, unregulated, and drains a catchment area of approximately 16 000 km^2 of subarctic fell country into the Barents Sea. The first test site is located near the Tana Bru (Fig. 1) and includes the only part of the river where the deep-water radiance could be retrieved, and hence allows a test of the estimation against observed values. The riverbed substrate at the test site consists of rocks in deep areas with strong current, and some sand in the shallows where the current is weaker.

The Pulmankijoki is a meandering, unregulated and ungauged tributary to the Tana. This site was chosen because it is optically shallow and it conforms better to the model assumptions than the deeper Tana Bru site. Importantly, there was also good data available for that site. Bathymetric models were built of one meander bend upstream of Lake Pulmanki. At the test site, the river is about 20 m wide during summer low flow and the riverbed consists of sandy sediments. Kasvi *et al.* (2013) describe the geomorphology of this study site in great detail.

Outside the spring flood, the water in both Tenojoki and Pulmankijoki is very clear for high-latitude rivers. It is worth considering, however, that this environment is more challenging for optically-based bathymetry modelling than, for instance, a tropical ocean, which has an attenuation depth of several tens of metres (e.g., Lee *et al.* 1999, Dierssen *et al.* 2003). The relatively low angle of solar zenith at these latitudes (70.2°N), even during the summer, is another factor that contributes to this environ-

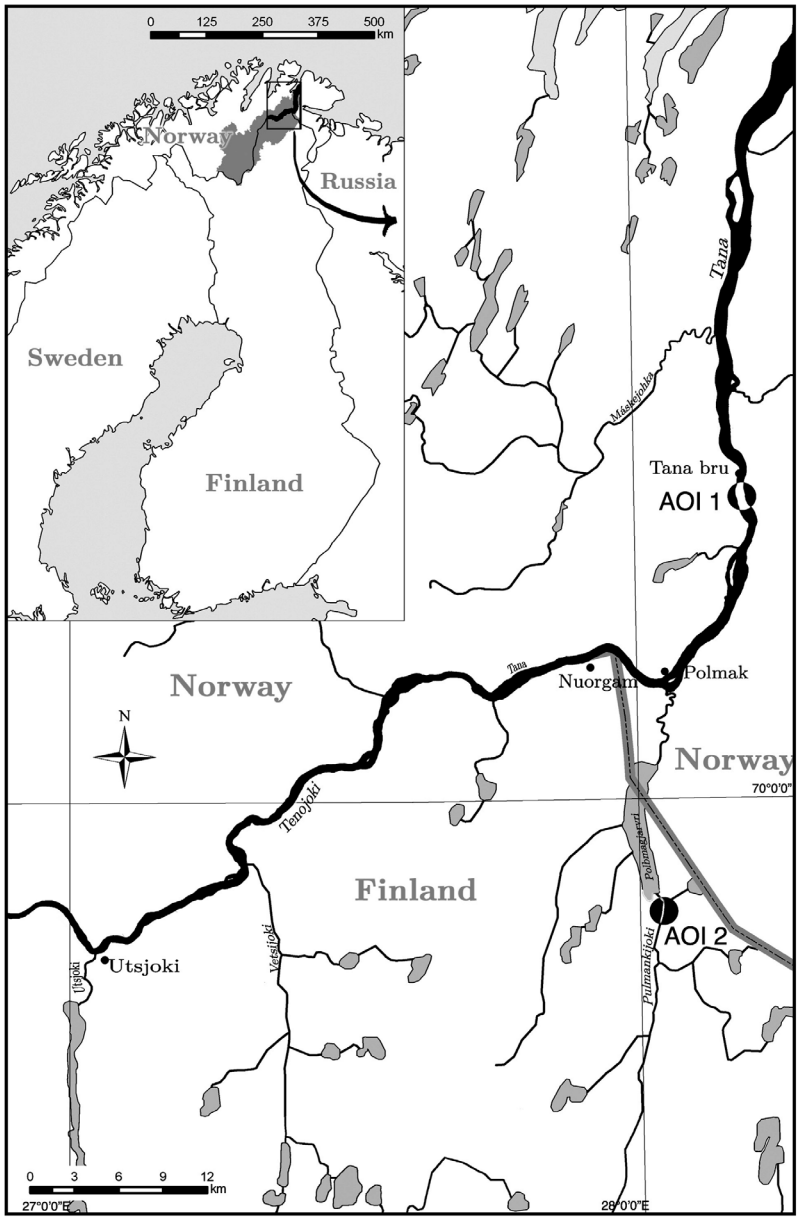

Fig. 1. Map showing the location of the areas of interest at Tana Bru (AOI 1) and Pulmankijoki (AOI 2) highlighted in negative colours. The location of the Polmak gauging station is also indicated.

ment approaching the limits of applicability of this technique.

Material and methods

At the Tana Bru site, aerial images in true colour RGB with a ground resolution of 0.5 m (Fig. 2) produced by TerraTec AS in July 2005 and georectified by the Norwegian Mapping Authority were used in conjunction with field data gathered in 2009 using a Furuno FCV-600L dual frequency sonar (accuracy ±0.1 m) coupled with a Thales real-time kinematic GPS (RTK-GPS) system (accuracy ±0.02 m) mounted to a zodiac. The time gap between the date of image acquisition and the ground data measurements is less than ideal. However, no more recent images were available for the area. Flener *et al*. (2012) found the time gap to affect the model results

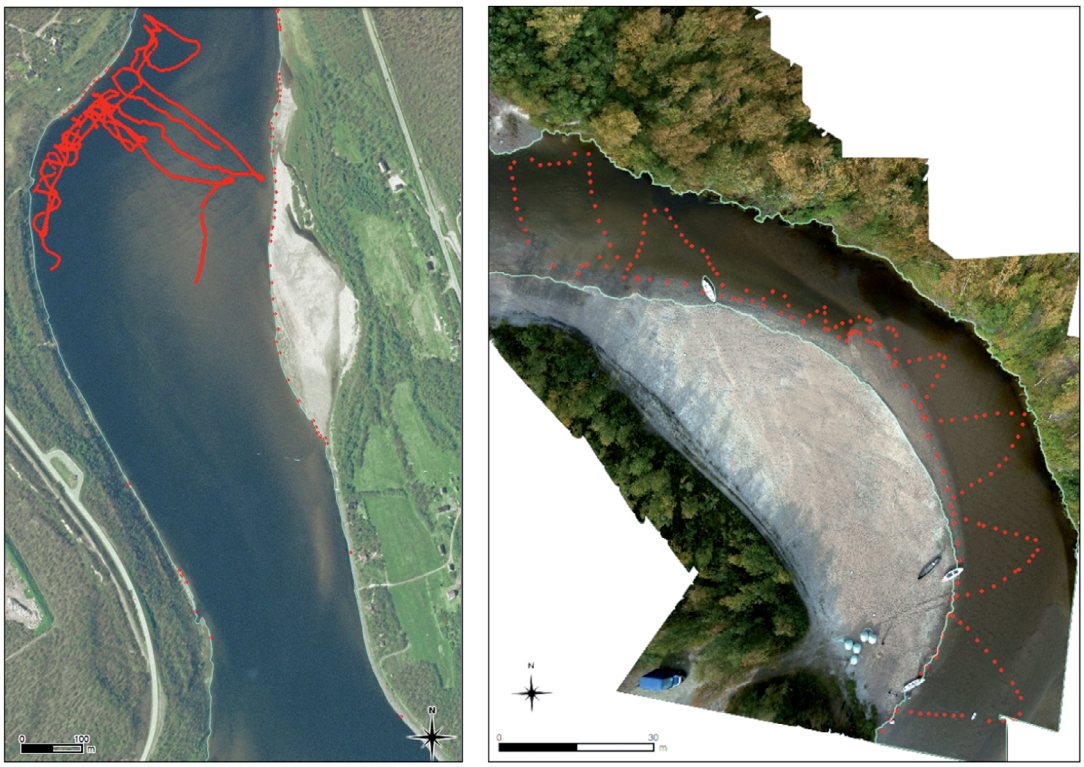

Fig. 2. Aerial images of the study areas: Tana Bru RGB 0.5-m-resolution image (right) and Pulmankijoki RGB 0.05 m UAV-based image mosaic (left). The ground data points used for the estimation of deep-water radiance as well as bathymetric model calibration are shown in red.

less than the contiguity of the ground data, and, given the results previously achieved by the same authors using data from the same flight campaign on a different location on the Tana river, and given that the rocky riverbed at the study site is fairly stable, these data were deemed adequate for this test.

The shoreline was manually digitised and used to extract the river area from the image. The measured water depths were adjusted to the water level of the day of image acquisition using data from the Polmak discharge gauging station. Polmak, located about 15 km upstream of the study site, is the most downstream gauging station on the Tana river and provides daily discharge and water level data. Both the aerial images and the ground data were gathered during summer low-discharge conditions. The water level on the flight day was 1.7 m with a discharge of 226.63 m^3 s^{-1}; on the day field data was gathered the water level 1.33 m with a discharge of 142.08 m^3 s^{-1}. Measurement errors were filtered from the depth point dataset, and the measured depths were systematically adjusted to the water level of the flight day. Since much of the shoreline is covered by vegetation, only those shoreline points that contained wetted riverbed were included in the model estimation. In total, 1875 points were used for calibrating and checking the models at Tana Bru. The Secchi depth measured in August 2009 at the Tana Bru site was 4.75 m, and the water depth at the measurement location was 6.2 m, the deepest point found in the lower half of the Tana river. The deep-water radiance values selected manually from the image according to the method suggested by Lyzenga (1981) at this site were R = 34, G = 62, B = 83 DN. These values from the same site were successfully used in bathymetric modelling on the Tana river in a previous study (Flener *et al*. 2012).

At the Pulmankijoki site, low-altitude RGB images with a ground resolution of 0.05 m

(Fig. 2) were acquired during 2010 using an unmanned aerial vehicle (UAV) (Flener *et al*. 2011), alongside 192 RTK-GPS-based riverbed elevation measurements covering virtually the entire spectrum of depths at that location. Depth values were calculated using an interpolated water surface based on RTK-GPS points. The images were mosaicked and georectified by the Finnish Geodetic Institute. The time gap between the flight and ground data was two days, and the depth values were adjusted to the time of flight using continuous water level data at the study site measured by automatic level logger during the field campaign.

Bathymetric maps were computed based on both the manually selected L_{si} values and the estimated values. After findings of Winterbottom and Gilvear (1997), Legleiter *et al*. (2004), Carbonneau *et al*. (2006) and Flener *et al*. (2012), I computed the depth models using the red and green bands only. Analogous to the deep-water parameter estimation, I cross-validated the model using 100-fold random sub-sampling using 70% of the points as the training set and 30% as the test set. The final model regression was created from the means of the regression coefficients of the training sets of the 100 model runs. For each model run, the result of the test set was validated against the corresponding measured data, producing the following statistics: RMSE, r^2, minimum, mean and maximum depth. The means of these cross-validation result statistics were used to assess the error of the model results. I produced the following models:

— At both locations, one model using L_{si} values automatically estimated using the above-described algorithm.
— At Tana Bru, one model using the manually selected L_{si} values (in Pulmankijoki it was not possible to manually choose these values since no deep enough area exists at that study site).
— At both locations, one model without subtracting L_{si} values ($L_{si} = 0$), i.e. assuming non-riverbed-radiance to be negligible.

The models are evaluated by comparing the root mean square error (RMSE), calculated as:

$$\mathrm{RMSE} = \sqrt{\frac{1}{n}\sum_{i=1}^{n}\left(D_{\mathrm{mi}} - D_{\mathrm{fi}}\right)^2} \qquad (3)$$

where D_{mi} is modelled depth at a measured point location and D_{fi} is field-measured depth at the same location, using the above-described cross-validation method. Moreover, the ability of the models to represent minimum, mean and maximum depths measured at each site is analysed. Furthermore, following the reasoning of Fonstad and Marcus (2005), visual assessment of the ability of the models to produce plausible-looking riverbeds that agree with the classical asymmetric model of a river without abrupt changes in depths was performed as well.

Results

When analysing the data for the Tana Bru site, the estimated L_{si} values (Table 1) are very close

Table 1. Estimation results and accuracy statistics for all models. The deep-water radiance values (L_{si}) for the red and green bands based on automatic estimation, manual selection and assumed negligible ($L_{si} = 0$) are listed. Root mean square error (RMSE) along with r^2 of the bathymetric regression and minimum (D_{min}), mean (D_{mean}) and maximum (D_{max}) modelled depths give an indication of the accuracy of the different bathymetric models produced and their ability to represent the depth spectrum found in the river (measured points).

Location	L_{si} source	L_{sRED}	L_{sGREEN}	RMSE	r^2	D_{min}	D_{mean}	D_{max}
Tana Bru	measured points					0	3.07	6.78
Tana Bru	automatically estimated	33	57	1.18	0.60	–0.46	3.16	6.45
Tana Bru	manually selected.	34	62	1.18	0.60	–0.49	3.17	6.63
Tana Bru	assumed negligible	0	0	1.20	0.58	–0.48	3.16	5.44
Pulmanki	measured points					0.03	0.36	0.84
Pulmanki	automatically estimated	2	3	0.12	0.75	0.04	0.36	0.90
Pulmanki	assumed negligible	0	0	0.12	0.75	0.03	0.36	0.89

to the values that were manually selected according to Lyzenga (1981). Correspondingly, the bathymetric maps produced for the Tana Bru site (Fig. 3), using estimated (Fig. 3A) and manually selected (Fig. 3B) L_{si} values, reveal little difference between the two methods of acquiring L_{si} and both models represent a plausible-looking river bed. Assuming L_{si} to be negligible results in a shallower bathymetric model (Fig. 3C). In order to get another perspective on the results, a transect was cut through a riverbed interpolation along a sonar line crossing the river. Figure 4 shows a cross-section of the three models at Tana Bru compared with a reference line interpolated from field-measured depth points. This reveals little difference between the three models, apart from the shallow area below 1 m near the left bank, which the $L_{si} = 0$ model estimates to be shallower than the estimated or manually selected L_{si} models do. The summary statistics (Table 1) also indicate that model ignoring deep-water radiance produces lower maximum depths than the other models. This is the only statistic that shows a difference greater than the uncertainty of the measured data. While roughly representing the asymmetric transect of the river, all three models fail to follow the reference transect below 2 m of depth.

The effect of the linearization achieved by applying Eq. 2 to the DN values of both the red and the green bands is illustrated in Figure 5. DN values as well as the X_i values computed using the different methods of obtaining L_{si} are plotted against measured depths. The gap in the data that is visible in these plots is due to the technical limitation of the sonar operating in water shallower than 0.6 m combined with the required water level adjustments. These plots reveal that there is very little relation between DN and depth below 2 m, suggesting a saturation of the radiance signal below this depth. While Lyzenga's algorithm manages to linearize the data to some extent, the resulting relationship is clearly not linear in this case. This is also reflected in the relatively low r^2 values (*see* Table 1) that indicate that the combined effect of the X_i values only explains 60% of the variation in depth. The automatic estimation algorithm terminated due to X_i reaching 0 before a perfect correlation could be achieved. The resulting X_i values based on the estimated L_{si} of red = 33 and green = 57 are very similar to the ones based on the manually selected L_{si} of red = 34 and green = 62, with correlation coefficients of X_i to depth of –0.77 for both methods in the red band and –0.71 in the green band. The correlation coefficients of X_i to depth were marginally lower when assuming L_{si} to be negligible, at –0.75 and –0.69 for red and green respectively.

The accuracy in terms of cross-validated RMSE (Table 1) is identical for the first two models, and the difference in RMSE of the $L_{si} = 0$ model to the other two models is well within the measurement error range of the field data. The error of all three models, at over one metre, is fairly large.

At the Pulmankijoki study site, two bathymetry models were produced, one using automatically estimated L_{si} and one ignoring L_{si} (Fig. 6). The automatic calibration algorithm terminated early due to spreading residuals, giving $L_{\mathrm{sRED}} = 2$ and $L_{\mathrm{sGREEN}} = 3$. Because these values are close to 0, the bathymetric map produced using the automatically estimated L_{si} is nearly identical to that ignoring L_{si}. The transect plot (*see* Fig. 7) also shows both models to be virtually identical. The bathymetric models represent a complete transect, whereas the reference line is an interpolation of 10 RTK-GPS points that do not include the right bank, and hence a coarser approximation of the riverbed than the reference line in Figure 4. Considering this, the models are in fairly good agreement with the reference transect.

The automatically estimated L_{si}-based X_i values have a slightly weaker correlation with depth than the DN values, whereas the $L_{si} = 0$ based X_i values have the same correlation to depth as the DN values (Fig. 8). The cross-validated RMSE for both models is 0.12. The summary statistics show that in Pulmanki, the minimum depth estimated is identical to the measured minimum (which differs from zero due to the water level adjustment to the flight time, mentioned earlier) in case of the $L_{si} = 0$ based model and within the error range of the RTK-GPS in case of the other model. The means of the modelled depths are identical to the mean of measured depths whereas the maxima are slightly overestimated.

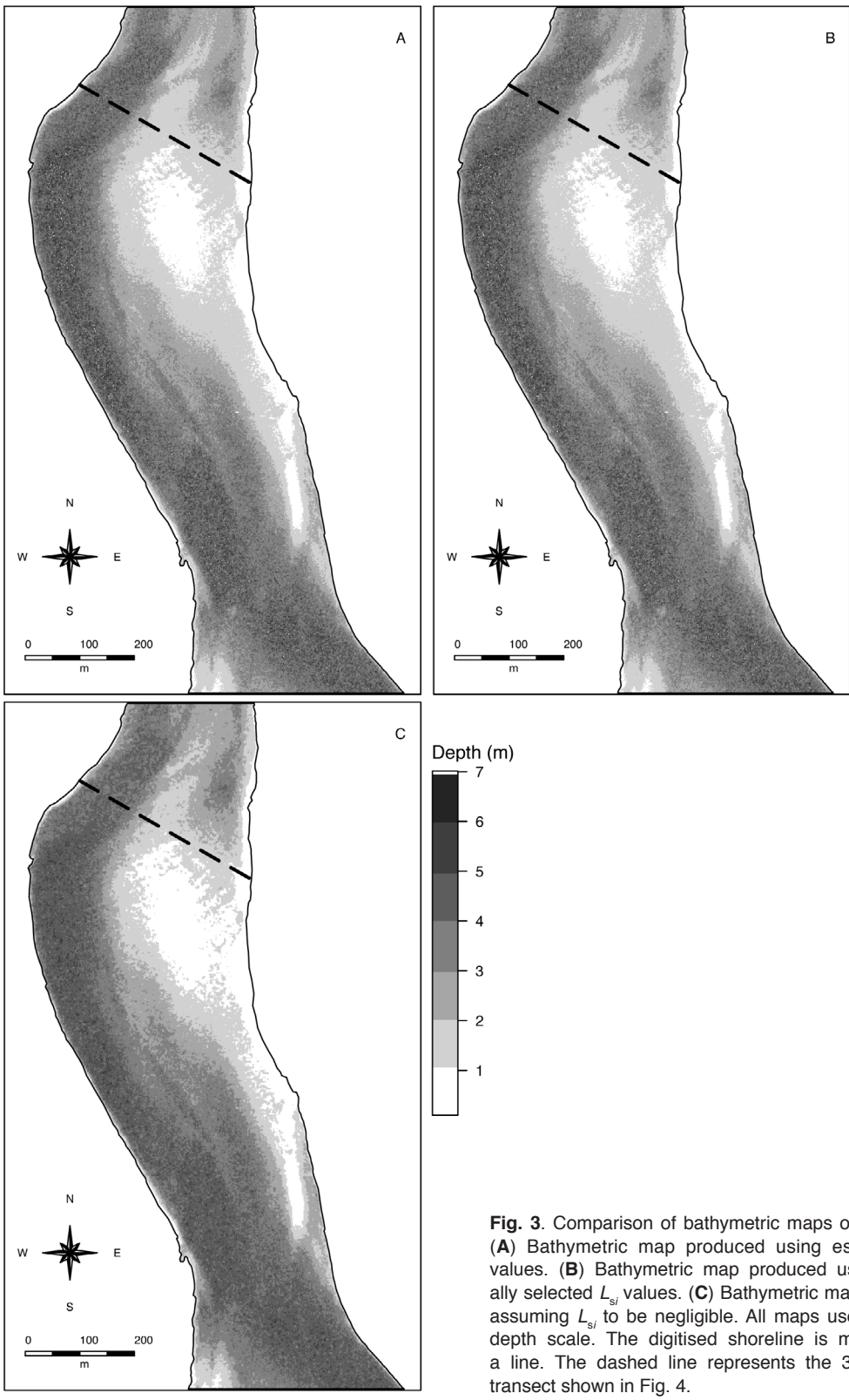

Fig. 3. Comparison of bathymetric maps of Tana Bru. (**A**) Bathymetric map produced using estimated L_{si} values. (**B**) Bathymetric map produced using manually selected L_{si} values. (**C**) Bathymetric map produced assuming L_{si} to be negligible. All maps use the same depth scale. The digitised shoreline is marked with a line. The dashed line represents the 365 m long transect shown in Fig. 4.

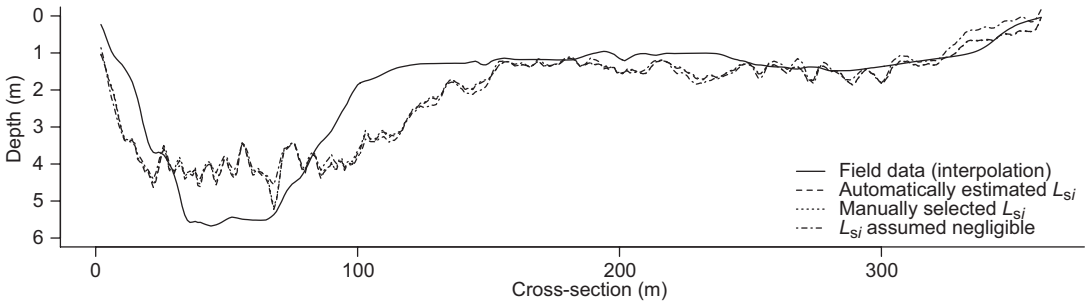

Fig. 4. Transect plot showing the results of the Lyzenga model at Tana Bru using automatic L_{si} estimation, manual L_{si} selection and L_{si} assumed negligible. All lines were smoothed with a moving average filter. The plot shows that there is no discernible difference between the model based on automatically estimated L_{si} and the one based on manually selected L_{si}. The reference line is an interpolation along the line shown in Fig. 3.

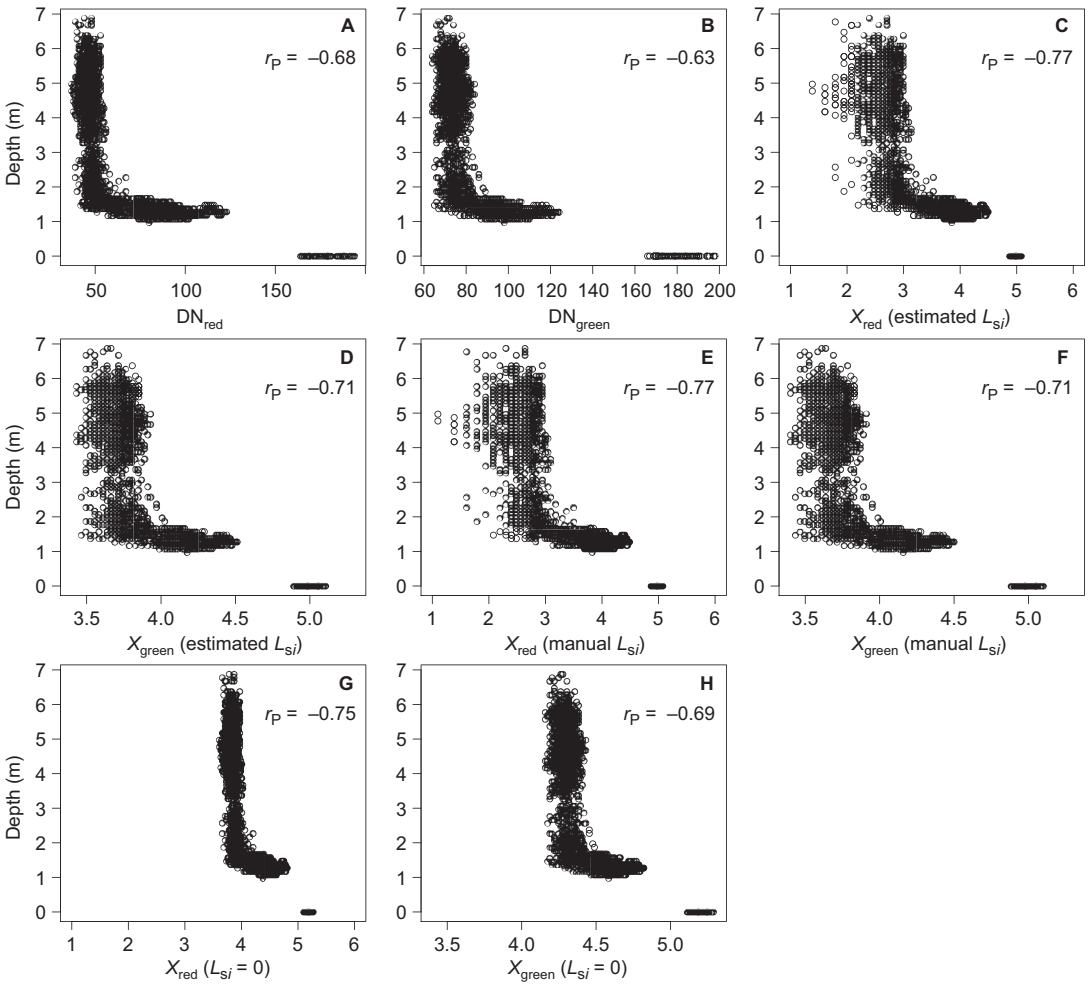

Fig. 5. DN_{red} and X_{red} plotted against depth and DN_{green} and X_{green} plotted against depth for the Tana Bru. (**A** and **B**) DN values plotted against depth, (**C** and **D**) deep-water corrected X values calculated using automatically estimated L_{si}, (**E** and **F**) manually selected L_{si}, and (**G** and **H**) L_{si} assumed negligible (L_{si} = 0). r_P = Pearson's correlation coefficient.

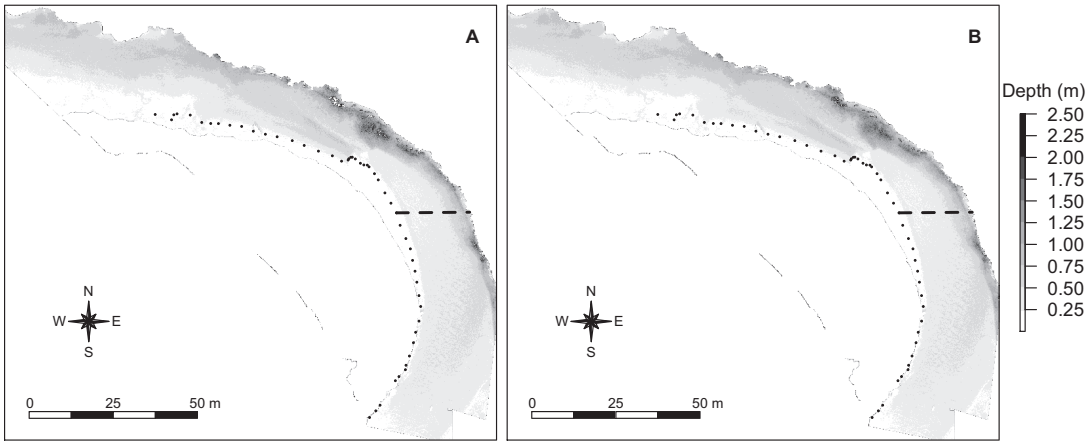

Fig. 6. Comparison of bathymetric maps of Pulmankijoki. (**A**) Bathymetric map produced using estimated L_{si} values. (**B**) Bathymetric map produced assuming L_{si} to be negligible. Both maps use the same depth scale. The points indicate the RTK-GPS-measured shoreline. The dashed line represents the 21.7 m long transect shown in Fig. 7.

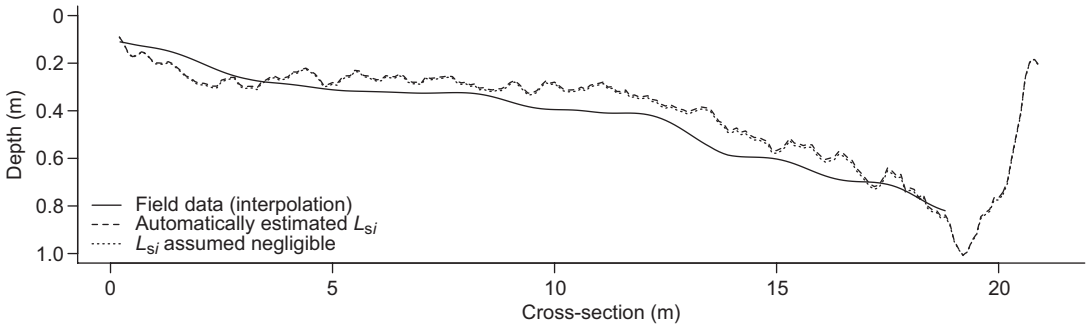

Fig. 7. Transect plot showing the results of the Lyzenga model at Pulmankijoki using automatic L_{si} estimation and L_{si} assumed negligible. All lines were smoothed with a moving average filter. The reference line is an interpolation of measured points without extrapolation (hence the line does not cover the entire transect), sampled along the line shown in Fig. 6.

Discussion

The results show that the automatically estimated deep-water radiance values and the manually selected values in Tana Bru are very close. The identical RMSE values and near minima, means and maxima (Table 1) indicate that the estimation algorithm works. Since the manually selected values are not without potential for error or bias, the automatic estimation of deep-water radiance values can be considered a preferable method because it produces reproducible and objective results.

While both deep-water-corrected models slightly underestimate the maximum depth relative to the field-measured data, the model that assumes deep-water radiance to be negligible is the only one in which this difference (1.34 m) exceeds RMSE of the model.

On the other hand, the plots of the original DN values (Fig. 5) show that there is little relation the between DN values and depth below 2 m, possibly indicating saturation of the radiance signal, and consequently, the plots of the X_i values show large scatter in the deeper areas. Therefore, the bathymetric model cannot be expected to deliver high accuracy in the deeper parts. Using *in situ* field spectrometry, Gilvear *et al*. (2007) noted a decrease in classification accuracy with increasing depth. The models also overestimate depth between two and four metres. While this may be due to a change in the riverbed

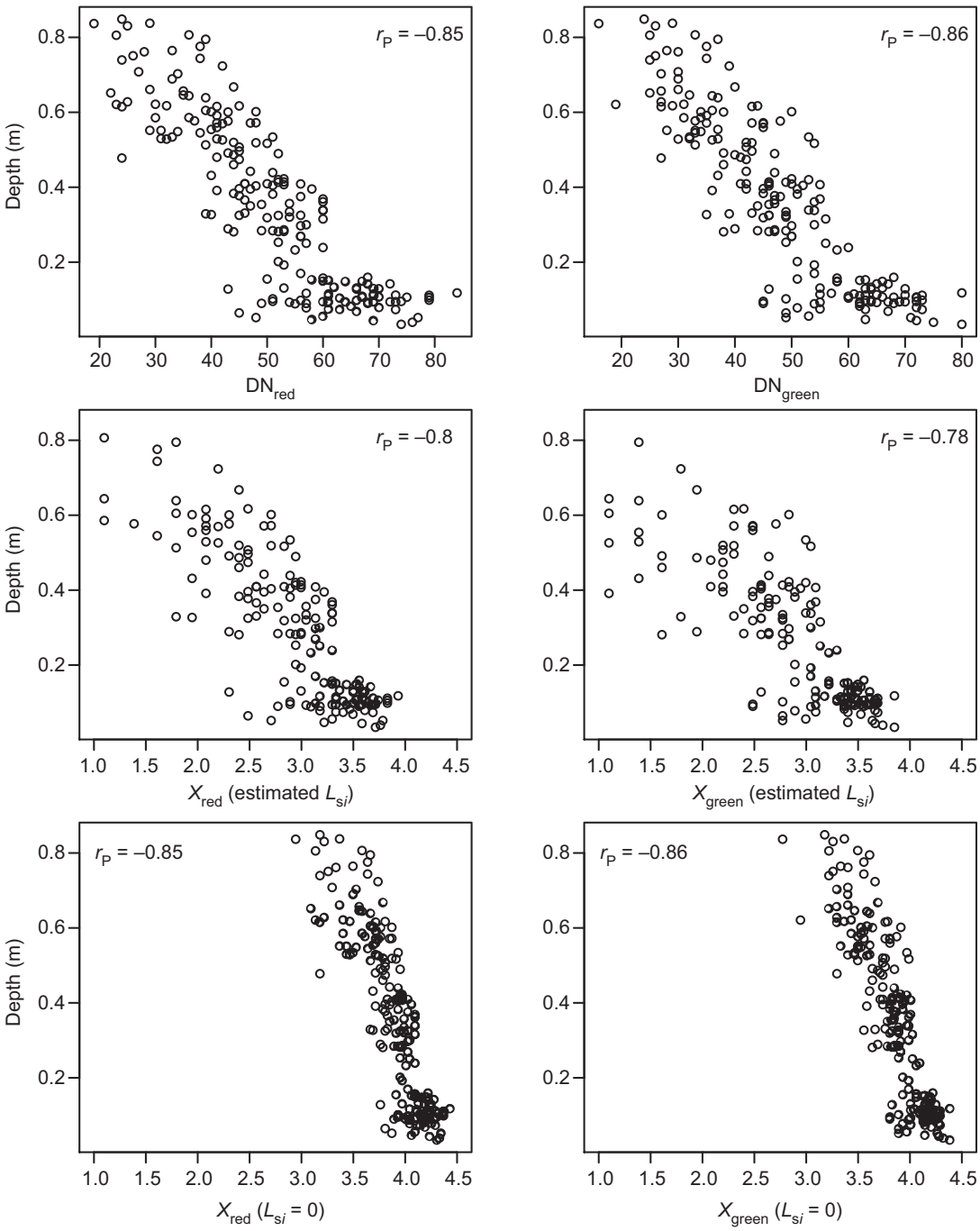

Fig. 8. DN_{red} and X_{red} plotted against depth (left column) and DN_{green} and X_{green} plotted against depth (right column) for Pulmankijoki. DN values plotted against depth (top row), deep-water corrected X values calculated using automatically estimated L_{si} (middle row) and L_{si} assumed negligible (L_{si} = 0) (bottom row). r_P = Pearson's correlation coefficient.

during the flight–field-campaign time interval, the stable nature of the rocky river bed suggests that it is more likely due to the lack of relationship between DN and depth below 2 m. This is

likely due to the challenging light conditions for remote sensing at these high latitudes, especially under water. Poor riverbed illumination can cause the effect of depth changes on brightness values to decrease beyond a detectable level (Gilvear *et al*. 2007). Legleiter *et al*. (2004) and Legleiter *et al*. (2009) discussed the limitations of attenuation-based bathymetric modelling due to the saturation of certain bands at depths shallower than the maximum depth to be modelled. They emphasise the need to find a balance between the sensitivity of a wavelength to water depth and the rate at which it becomes saturated, in particular in regard to selecting bands from multispectral data for bathymetric modelling. That means that bands of which the DN stops changing with depth at depths shallower than the maximum depth to be modelled are problematic. Legleiter *et al*. (2004) showed that the ability to differentiate bathymetric detail is inherent to the radiometric resolution of the sensor and also decreases with increasing depth. The 8-bit radiometric resolution of the images used in this study therefore determines the maximum depth that can be modelled, even though the combination of two bands increases this range compared to using one single band.

The discrepancy between measured and modelled depths may also be due to possibly higher turbidity on the flight day than on the day Secchi depth was measured. Unfortunately, this cannot be verified retrospectively. Atmospheric effects may also play a role here, although the deep-water correction should account for those. However, considering that the relationship between DN and depth in the shallow areas is as expected according to the Beer-Lambert law, the results obtained at Tana Bru are pertinent. Furthermore, one aim of this paper is to establish whether the method of estimating deep-water radiance yields results comparable to manually selecting that parameter, rather than assessing the bathymetric model itself (cf. Flener *et al*. 2012, for a discussion on the applicability of the Lyzenga model in subarctic rivers).

Even while considering the limitations of the model in deeper water, the results also indicate that, at least in this case, assuming deep-water radiance to be negligible results in a model that is less able to represent the deep part of the river than the models utilising deep-water correction.

Since optical bathymetric modelling relies on the light reflected by the riverbed, it is not feasible beyond Secchi depth. In fact, unless the riverbed is white, the maximum depth that can be modelled successfully would be shallower than the Secchi depth. In this case, there is little relation between depth and radiance values beyond about half Secchi depth (Fig. 5). This explains the rather poor correspondence of the resulting depth model to the measured data, expressed as root mean square error (Table 1). In a study comprising a range of water depths at sea, Pahlevan *et al*. (2006) also found the Lyzenga model to perform poorly in deeper water.

The Pulmankijoki site was used in order to verify the deep-water radiance estimation algorithm in conditions that better meet the requirements of the bathymetric model. The depth range does not exceed Secchi depth here and the substrate is fairly homogenous. These conditions are reflected in much lower RMSE values than for Tana Bru. Figure 8 shows that there is a clear relationship between depth and radiance over the entire spectrum of measured data.

There are two interesting conclusions to be made about the models in Pulmankijoki. First, the deep-water radiance estimates are very low. This is due to the routine that checks against creating a condition resulting in impossible values due to logarithms being computed of negative numbers, at least on the input data. The other — and more important — conclusion is that there is virtually no difference between the model including the estimated L_{si} and the one assuming L_{si} to be negligible. This indicates that, in this case, the deep-water radiance parameter can indeed be ignored and Lyzenga's X can be computed by simply taking the natural logarithm of DN. However, one has to bear in mind that the Pulmankijoki model was based on very low altitude (40–50 m) UAV-based aerial photography. Considering that the deep-water correction also accounts for atmospheric effects, it may still be advisable to use the automatically estimated deep water radiance value when modelling shallow rivers based on regular aerial imagery that is typically acquired from much higher altitudes where atmospheric effects may not be ignored.

It should also be noted that r^2 for both models in Pulmanki, at 0.75, is greater than that for

Tana Bru, but this still leaves 25% of the effect of variation in depth unexplained by the model. Some of this is probably due to slight variation in the substrate — even though the substrate is very homogenous for a natural river — or even due to shadowing effects of sand ripples and small dune features on the riverbed caused by the relatively low incidence angle of solar rays at these latitudes.

Considering the riverbed topography of both test sites and the results of the bathymetric models, it is clear that depth retrieval from optical images is most effective in shallow waters. This finding is in line with the theoretical analysis of Legleiter *et al*. (2004).

While the Lyzenga model can clearly deliver high accuracy results within its range of assumptions, such as in the case of Pulmankijoki, the substrate homogeneity requirement can be difficult to meet when modelling larger areas. Algorithms using ratios of different spectral bands have been developed in coastal areas (e.g. Dierssen *et al*. 2003, Stumpf and Holderied 2003) aiming at overcoming the influence of sediment variability on depth estimates. Similarly, Legleiter *et al*. (2004) presented a ratio-based algorithm in a river setting that, in addition to being robust relative to substrate and atmospheric variability, boasted the advantage of not requiring deep-water radiance. While that property remains true for their algorithm, the estimation method presented here removes that disadvantage from Lyzenga's (1981) original algorithm. Whereas Lyzenga's bathymetry algorithm may still be sensitive to variability in bottom albedo, Legleiter *et al*. (2004) point out that depth is generally the primary control on measured radiance and they found both ratio-based and linear-transform based depth values correlated strongly with measured depths. Gilvear *et al*. (2007) concluded that, although band-ratioing can give good results, it does not always give the best results and they suggest that workers should also examine the accuracy obtainable by Lyzenga's algorithm. While the algorithm presented here does not necessarily improve the accuracy of the Lyzenga (1981) model results, it potentially widens its range of applicability as well as increasing its objectivity. The deep-water radiance algorithm can even be used with single-band models, which Lyzenga's algorithm is able to handle, as opposed to ratio-based models.

Conclusion

The results of this study indicate that the estimation of the deep-water radiance parameter is possible, and that the resulting depth models produced are of similar accuracy to those that have previously been achieved in river waters reaching several metres of depth. Deep-water radiance seems to have little effect on the results of the bathymetric model in optically shallow water. That parameter can be ignored in very shallow water such as the Pulmankijoki site, with depths up to one metre, at least when the modelling is based on very low altitude photography. However, with higher altitude photography and/or deeper water, accuracies achieved with the estimated L_{si} as compared with those with the observed L_{si} suggest that the reproducible automatic estimation algorithm can replace the more subjective manual selection method. This new estimation method has the potential to expand the applicability of the Lyzenga depth model to shallow rivers where the lack of deep water would have precluded its use so far, at least without the use of spectrometry. The validated assumption of deep-water radiance being negligible in optically shallow water may also be of practical use when modelling bathymetry in very shallow water. This opens up a host of opportunities for river researchers making it possible to create contiguous surface depth models of shallow riverbeds without the need for interpolation. These models can provide valuable input data to hydraulic models used for instance in fluvial geomorphology, fish habitat modelling and hydraulic engineering. Multi-temporal remote-sensing based bathymetry models also allow change detection in fluvial geomorphology.

Acknowledgements: This study was funded by Tekes (GIFLOOD research project), Maj and Tor Nessling Foundation (FLOODAWARE research project) and the Academy of Finland (RivCHANGE research project). The aerial photography data sets were supplied at an institutional price level by Norsk Eiendomsinformasjon AS. Fieldwork was supported by the Kevo Subarctic Research Station and the field assistance of Petteri Alho, Eliisa Lotsari and Elina Kasvi is grate-

fully acknowledged. I am also indebted to Juha Hyyppä, Anttoni Jaakkola and Anssi Krooks for their work acquiring and processing the UAV imagery. Finally, I would like to thank the reviewers for their constructive criticism and comments of the manuscript.

References

Alho P. & Mäkinen J. 2010: Hydraulic parameter estimations of a 2D model validated with sedimentological findings in the point bar environment. *Hydrological Processes* 24: 2578–2593.

Bates P., Marks K. & Horritt M. 2003: Optimal use of high-resolution topographic data in flood inundation models. *Hydrological Processes* 17: 537–557.

Bryant R.G. & Gilvear D.J. 1999: Quantifying geomorphic and riparian land cover changes either side of a large flood event using airborne remote sensing: River Tay, Scotland. *Geomorphology* 29: 307–321.

Carbonneau P.E., Lane S.N. & Bergeron N. 2006: Feature based image processing methods applied to bathymetric measurements from airborne remote sensing in fluvial environments. *Earth Surface Processes and Landforms* 31: 1413–1423.

Conger C., Hochberg E., Fletcher C.III & Atkinson M. 2006: Decorrelating remote sensing color bands from bathymetry in optically shallow waters. *IEEE transactions on Geoscience and Remote Sensing* 44: 1655–1660.

Dierssen H., Zimmerman R., Leathers R., Downes T. & Davis C. 2003: Ocean color remote sensing of seagrass and bathymetry in the Bahamas Banks by high-resolution airborne imagery. *Limnology and Oceanography* 48: 444–455.

Flener C., Jaakkola A., Hyyppä J. & Alho P. 2011: Very high resolution bathymetric modelling from low altitude UAV-based imagery. *Geophysical Research Abstracts* 13, EGU2011-405.

Flener C., Lotsari E., Alho P. & Käyhkö J. 2012: Comparison of empirical and theoretical remote sensing based bathymetry models in river environments. *River Research and Applications* 28: 118–133.

Gilvear D., Hunter P. & Higgins T. 2007: An experimental approach to the measurement of the effects of water depth and substrate on optical and near infra-red radiance: a field-based assessment of the feasibility of mapping submerged instream habitat. *International Journal of Remote Sensing* 28: 2241–2256.

Horritt M. & Bates P. 2002: Evaluation of 1D and 2D numerical models for predicting river flood inundation. *Journal of Hydrology* 268: 87–99.

Kasvi E., Vaaja M., Alho P., Hyyppä H., Hyyppä J., Kaartinen H. & Kukko A. 2013: Morphological changes on meander point bars associated with flow structure at different discharges. *Earth Surface Processes and Landforms* 38: 577–590.

Lane S. 2000: The measurement of river channel morphology using digital photogrammetry, *Photogrammetric Record* 16: 937–957.

Lane S., Westaway R. & Hicks D. 2003: Estimation of erosion and deposition volumes in a large, gravel-bed, braided river using synoptic remote sensing. *Earth Surface Processes and Landforms* 28: 249–271.

Lee Z., Carder K.L., Mobley C.D., Steward R.G. & Patch J.S. 1999: Hyperspectral remote sensing for shallow waters. 2. Deriving bottom depths and water properties by optimization. *Applied Optics* 38: 3831–3843.

Legleiter C., Roberts D., Marcus W. & Fonstad M. 2004: Passive optical remote sensing of river channel morphology and in-stream habitat: physical basis and feasibility. *Remote Sensing of Environment* 93: 493–510.

Legleiter C. & Roberts D. 2005: Effects of channel morphology and sensor spatial resolution on image-derived depth estimates. *Remote Sensing of Environment* 95: 231–247.

Legleiter C., Roberts D. & Lawrence R. 2009: Spectrally based remote sensing of river bathymetry. *Earth Surface Processes and Landforms* 34: 1039–1059.

Lotsari E., Veijalainen N., Alho P. & Kayhkö J. 2010: Impact of climate change on future discharges and flow characteristics of the Tana river, sub-arctic northern Fennoscandia. *Geografiska Annaler Series* 92A: 263–284.

Lyzenga D.R. 1981: Remote sensing of bottom radiance and water attenuation parameters in shallow water using aircraft and Landsat data. *International Journal of Remote Sensing* 2: 71–82.

Marcus W.A. & Fonstad M.A. 2008: Optical remote mapping of rivers at sub-meter resolutions and watershed extents. *Earth Surface Processes and Landforms* 33: 4–24.

Pahlevan N., Valadanzouj M.J. & Alimohamadi A. 2006: A quantitative comparison to water column correction techniques for benthic mapping using high spatial resolution data. In: Kerle N. & Skidmore A. (eds.), *ISPRS Commission VII Mid-term Symposium "Remote Sensing: From Pixels to Processes", Enschede, The Netherlands*, ISPRS, Copernicus Publications, pp. 286–291.

Stumpf R.P., Holderied K. & Sinclair M. 2003: Determination of water depth with high-resolution satellite imagery over variable bottom types. *Limnology and Oceanography* 48: 547–556.

Westaway R., Lane S. & Hicks D. 2003: Remote survey of large-scale braided, gravel-bed rivers using digital photogrammetry and image analysis. *International Journal of Remote Sensing* 24: 795–815.

Winterbottom S.J. & Gilvear D.J. 1997: Quantification of channel bed morphology in gravel-bed rivers using airborne multispectral imagery and aerial photography. *Regulated Rivers-Research & Management* 13: 489–499.

Wright A., Marcus W. & Aspinall R. 2000: Evaluation of multispectral, fine scale digital imagery as a tool for mapping stream morphology. *Geomorphology* 33: 107–120.

Appendix

Pseudo-code of deep-water radiance estimation algorithm as performed on each band separately.

```
seed = 0
Xi = 999
while correlationCoefficient != –1 and min(Xi) > 0 do
        X = ln(DN – seed)
        linear.model(depth ~ X)
        if correlationCoefficient == –1 then
                DeepWaterRadiance = seed
                return DeepWaterRadiance
        else
                seed = seed + 1
                Xi = log(DN-seed)
        end if
end while
```